Electronic Supplementary Material

Efficient Bi-enzymatic Synthesis of Aldonic Acids

Lidija Tetianec[1], Irina Bratkovskaja[1], Vida Časaitė[2], Vidutė Gurevičienė[1], Julija Razumienė[1], Jonita Stankevičiūtė[2], Rolandas Meškys[2], Marius Dagys[1], Audrius Laurynėnas[1†]

1 *Department of Bioanalysis, Institute of Biochemistry, Life Sciences Center, Vilnius University, 7 Saulėtekio Ave, LT- 10257 Vilnius, Lithuania.*
2 *Department of Molecular Microbiology and Biotechnology, Institute of Biochemistry, Life Sciences Center, Vilnius University 7 Saulėtekio Ave, LT-10257 Vilnius, Lithuania.*
† Corresponding author.

Expression and purification of recombinant PQQGDH

E. coli DH5α strain was transformed with pASK-IBA3 (IBA GmbH, Göttingen, Germany) cloned glucose dehydrogenase gene (WP_002121021.1). Cells harboring plasmid were grown overnight in BHI (Oxoid, FisherScientific, Vilnius, Lithuania) medium supplemented with 50 mg/L ampicillin aerobically at 30°C, then 2 ml of night culture were transferred to 200 ml of the same medium, and cells were grown at 30°C with rotary shaking until optical density (OD_{600}) reached 0.8. Gene expression was induced by adding 200 µg/L anhydrotetracycline. The cells were incubated at 22 °C overnight, collected by centrifugation (20 min at 3,220 × g at 4°C), suspended in lysis buffer (10 mM Tris–HCl, pH 7.0) and disrupted by sonication (5 min at 22 kHz in ice-water bath, 40% of amplitude). Centrifugation-clarified lysates (16,000 *g* for 10 min) were loaded onto TOYOPEARL CM-650M (ToyoSoda, Tokyo, Japan) column equilibrated with the lysis buffer. Glucose dehydrogenase was eluted with 0–0.4 M NaCl gradient, fractions with glucose dehydrogenase activity were collected, concentrated, and dialyzed against 10 mM ammonium bicarbonate pH 7.8 buffer. Then the protein was dehydrated by lyophilization and stored at 4 °C. About 30 mg of enzyme was purified from 1 L of culture.

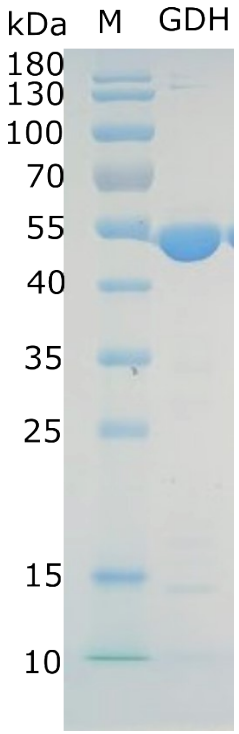

Figure S1. Purified PQQGDH in the 14 % SDS-PAGE.

Investigation of the PQQGDH reactivity with thionine

The reactivity of PQQ GDH with thionine was investigated spectrophotometrically by observing the decrease of thionine absorbance. For different thionine concentrations the different wavelengths were used: for concentrations lower than 20 μM the wavelength was 600 nm, for concentrations from 20 μM to 120 μM the wavelength was 500 nm, for concentrations higher than 120 μM the wavelength was 450 nm. The experimentally determined coefficients of molar absorbance (60 $mM^{-1}cm^{-1}$ at 600 nm, 7.4 $mM^{-1}cm^{-1}$ at 500 nm and 2.1 $mM^{-1}cm^{-1}$ at 450 nm) were used to calculate the concentration of thionine and the rate of the thionine reduction reaction. Glucose (10 mM) was used as the enzyme reducing substrate. The dependence of the thionine reduction rate on the thionine concentration was approximated by the Michaelis-Menten equation and the apparent parameters V_{max} and K_m were calculated. The bimolecular PQQ GDH and thionine reactivity rate constant was calculated as $V_{max}/(K_m*E_{PQQGDH})$, were E_{PQQGDH} – the concentration of PQQGDH.

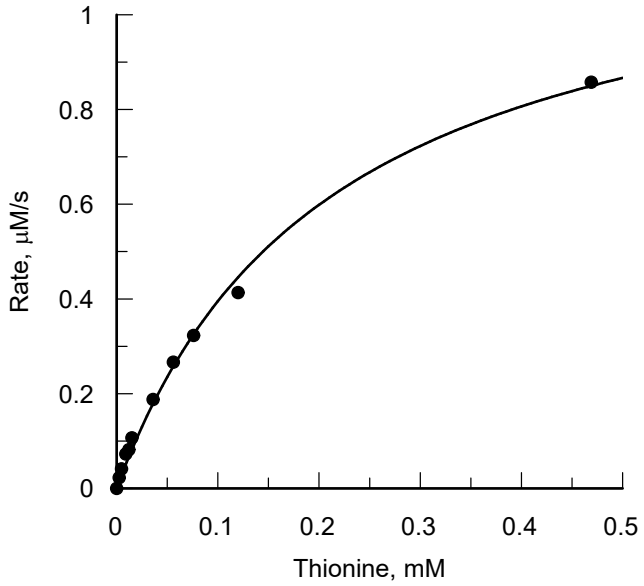

Fig. S2. The dependence of PQQGDH-catalysed thionine reduction rate on thionine concentration at pH 7, 10 mM glucose, 2.0 nM PQQGDH, anaerobic conditions.

The parameters of reactivity of saccharide substrates and PQQGDH

Thionine was used as the terminal electron acceptor in the reaction of PQQGDH-catalysed saccharide substrate oxidation. The concentration of thionine in the reaction mixture was 220 μM or 410 μM. The reduction of thionine was observed at 450 nm of wavelength in the presence of PQQGDH and various concentrations of saccharide substrate. For the calculation of the rate of thionine reduction the experimentally determined thionine extinction coefficient was used. The rate was normalized to the concentration of the PQQGDH in the reaction mixture [E_0]. The dependence of the normalized thionine reduction rate on the saccharide concentration (Fig. S3) was analysed by applying the equation X1:

$$v/[E_0] = S \cdot (V_{max}/[E_0])/(K_M + S\cdot(1+(S/K_i)) \quad \text{(X1)},$$

and the apparent parameters K_M, K_i and $V_{max}/[E_0]$ were calculated by fitting experimental data to the equation X1 using nonlinear numerical least squares fitting method.

The ratio of normalized V_{max} with K_M was considered as the parameter specifying the reactivity of the various substrates – the higher the value of the ratio – the better substrate reactivity. K_i – is the enzyme inhibition by the substrate constant. The concentration of the substrate at which the rate of thionine reduction was maximal (c_{opt}) was calculated as $\sqrt{K_M \cdot K_i}$.

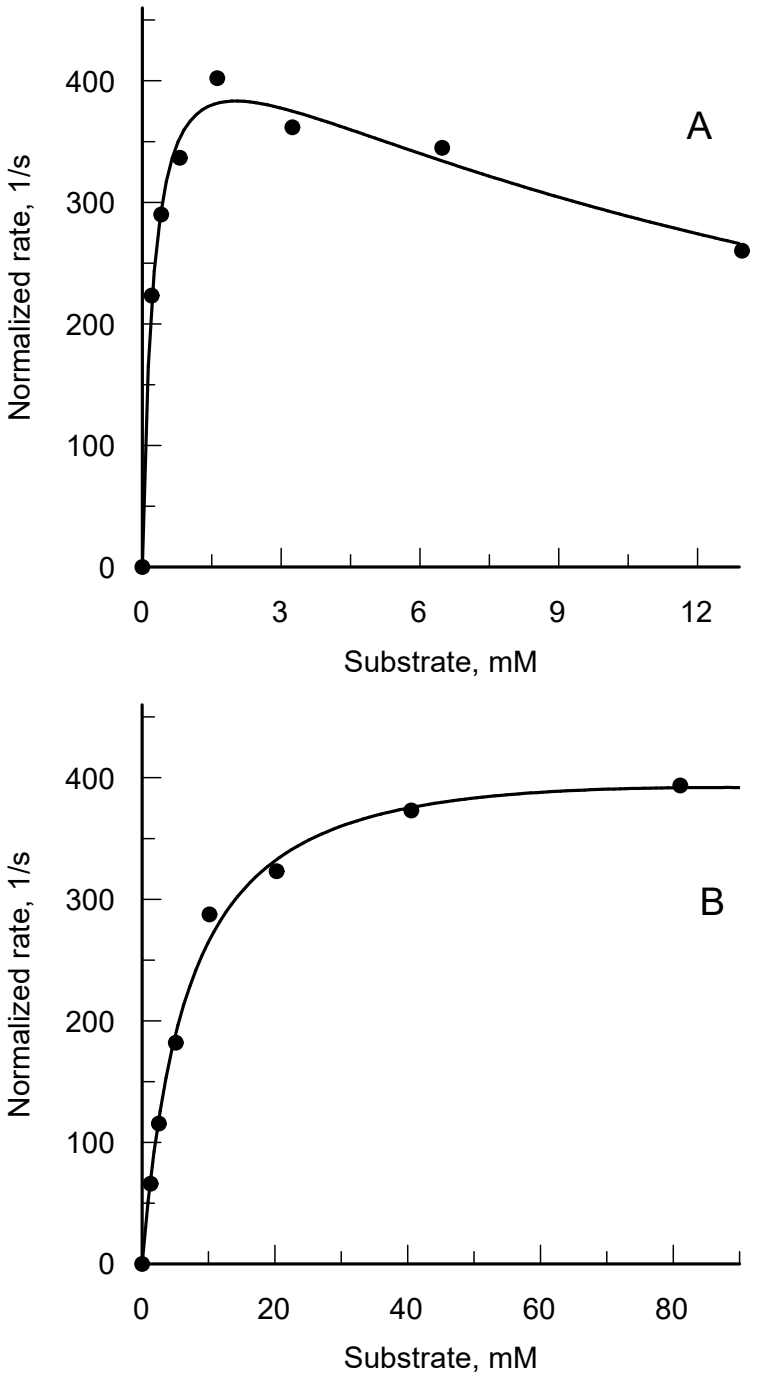

Fig. S3. The dependences of the PQQGDH-catalysed reaction rate on substrate concentration (cellobiose – A, xylose – B).

Scheme of the reactor

The addition of hydrogen peroxide, substrate and potassium hydroxide to the reactor mixture was performed in very small doses by using the precise dispenser (pump) developed by our team. The rate of hydrogen peroxide dosage was controlled by analysing the data of custom highly sensitive hydrogen peroxide and optical, oxidized mediator form, sensors. The rate of potassium hydroxide solution dosage was regulated considering the measurement of pH with pH electrode.

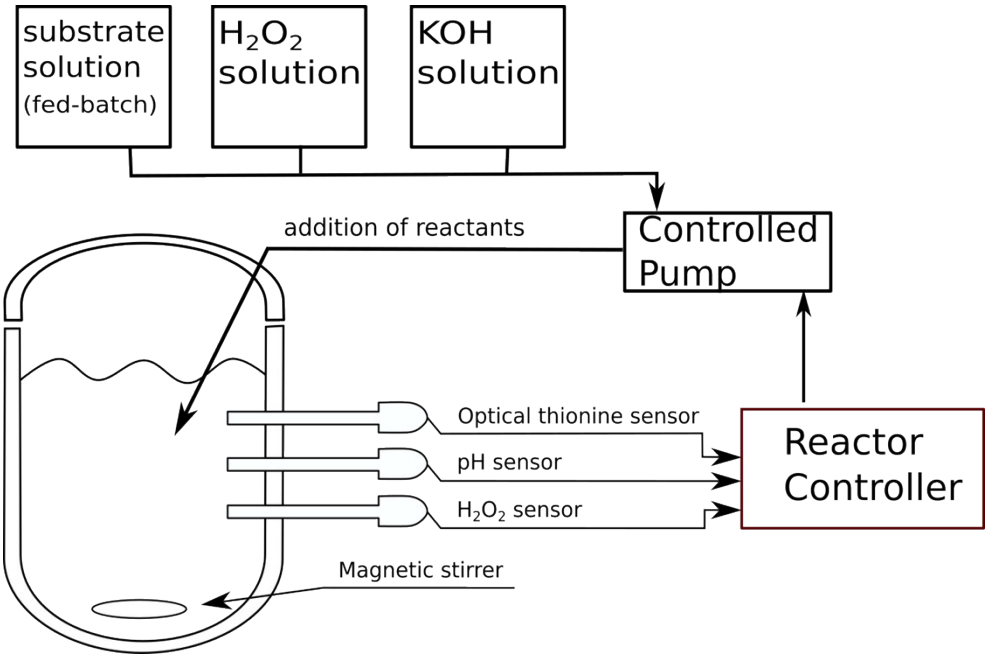

Scheme S1. Generalized scheme of the reactor system

Substrate addition to the fed-batch reactor

The substrate in fed-batch reactors was dozed at the same rate as hydrogen peroxide to compensate the substrate consumption equimolar to hydrogen peroxide addition. Regularly (not continuously) the concentration of substrate was checked by taking the probe and analysing with custom PQQGDH based substrate sensor. The sensor was constructed using PQQGDH as described in [1]. The sensor-determined fluctuations of substrate concentration were unrelated with its hydrogen peroxide linked oxidation but were related to the PQQGDH specificity for the substrate β-anomer, rate of substrate mutarotation and oxidation of leuco-thionine by dissolved oxygen. Part of the leuco-thionine was reoxidized by oxygen at slow rate. If the rate of the reaction of substrate (β-anomer) consumption was higher than the rate of mutarotation, the apparent decrease of substrate concentration (that in fact correlates with only β-anomer concentration) is observed. The observed decrease of substrate concentration due to both reasons was compensated by addition of deficient substrate to maintain the c_{opt} in fed-batch reactors. As the rate of conversion in reactor decreases and equalizes to rate of mutarotation, the substrate concentration exceeds c_{opt}. To solve this case, the concentration of substrate solution in dosage syringe was reduced until the concentration in reactor achieves c_{opt}.

Space-time yield of the reactors

Space-time yield (STY) is yield divided by the production time and reactor volume [2]. STY was calculated assuming the volume of the model reactor is 25 ml and the product of the reaction is the corresponding aldonic acid. For the mixture of galacto-oligosaccharides (GOS mixture) the average molecular masses of the initial substrate (341 g/mol) and of the corresponding acidic product (357 g/mol) were calculated assuming the mixture composition presented in Table S3. Yields of gluconolactone (Y_{H2O2} and Y_S) were calculated both from H_2O_2 consumed during reaction time (n_p) assuming equimolar oxidation of glucose and by subtracting leftover amounts of substrate in the end of the synthesis ($n_{S\ after}$, as measured with automatic glucose analyser EKSAN-Gm) from the total amount added during reaction duration (n_s). As it is seen from the Table S1, yields Y_{H2O2} and Y_S agree perfectly and gluconolactone production is equimolar with H_2O_2 consumption. Therefore, for other substrates (in Table S2) yields were calculated directly from amounts of H_2O_2 consumed during synthesis (n_p).

Table S1 Parameters of the glucose conversion reactors. (~6h production run; 0.8 nmol of PQQGDH, pH with asterisk – 0.4 nmol PQQGDH)

pH	[TH], mM	[$CaCl_2$], mM	n_S, *mmol*	n_p, mmol	$n_{S\ after}$, mmol	TTN_E x 10^{-6}	ATN_E x 10^{-3}, h^{-1}	STY, $g*L^{-1}*h^{-1}$	Y_{H2O2}, %	Y_S, %
8.0	0.41	100	5.7	5.7	0.14	7.1	1165	7.3	99	98
8.0	0.41	5	5.9	5.7	0.18	7.1	1146	7.2	97	97
7.0*	0.41	5	2.8	2.6	0.14	6.5	1049	3.3	95	95
8.0*	0.41	5	4.2	4.0	0.11	10.0	1586	5.0	96	97
7.0*	0.41	100	3.8	3.6	0.22	9.0	1450	4.6	96	94
8.0*	0.41	100	4.2	3.9	0.19	9.7	1573	4.9	93	95
8.0	0.22	100	3.9	3.8	0.040	4.7	760	4.8	97	99
8.0	0.22	100	4.0	4.0	0.040	4.9	810	5.1	99	99
7.0	0.22	100	3.3	3.3	0.062	4.2	672	4.2	98	98
8.0	0.22	5	2.8	2.7	0.12	3.3	557	3.5	96	96
7.0	0.22	5	2.1	2.0	0.094	2.5	390	2.5	95	96

Table S2 Parameters of the saccharides' conversion reactors

Substrate	Conditions	n_p, mmol	*Production time*, h	TTN_E x 10^{-6}	ATN_E x 10^{-3}, h^{-1}	STY, $g*L^{-1}*h^{-1}$	Y_{H2O2}, %
deoxyribose	pH 7.0; 5mM CaCl2; 0.22 mM TH; batch	0.97	6.6	0.065	9.85	0.88	45
lyxose	pH 7.0; 5mM CaCl2; 0.22 mM TH; batch	2.3	10.3	0.15	14.6	1.5	62
ribose	pH 7.0; 5mM CaCl2; 0.22 mM TH; batch	3.6	7.2	0.82	114	3.3	53
cellobiose	pH 7.0; 5mM CaCl2; 0.22 mM TH; fed-batch	0.69	6.6	1.3	197	1.5	81
lactose	pH 7.0; 5mM CaCl2;	0.94	6.8	1.3	191	2.0	82

	0.22 mM TH; fed-batch						
xylose	pH 7.0; 5mM CaCl2; 0.22 mM TH; batch	22	45.3	2.2	48.6	3.2	81
GOS mixture	pH 7.0; 5mM CaCl2; 0.22 mM TH; batch	1.3	6.0	0.43	72.5	1.7	44
deoxyribose	pH 7.0; 100mM CaCl2; 0.41 mM TH; batch	1.1	6.1	0.15	25	1.1	28
lyxose	pH 7.0; 100mM CaCl2; 0.41 mM TH; batch	0.97	6.2	0.18	29	1.0	19
ribose	pH 7.0; 100mM CaCl2; 0.41 mM TH; batch	5.5	6.3	1.0	159	5.8	48
cellobiose	pH 7.0; 100mM CaCl2; 0.41 mM TH; fed-batch	0.93	6.0	3.4	569	2.2	68
lactose	pH 7.0; 100mM CaCl2; 0.41 mM TH; fed-batch	0.95	6.0	3.5	575	2.3	69
xylose	pH 7.0; 100mM CaCl2; 0.41 mM TH; batch	10	6.1	1.8	300	10.9	92
galactose	pH 7.0; 100mM CaCl2; 0.41 mM TH; fed-batch	5.7	5.7	2.1	370	7.8	85
GOS mixture	pH 7.0; 100mM CaCl2; 0.41 mM TH; batch	1.7	6.1	0.61	100	4.0	35

Table S3. Composition of dry powder of mixture of galacto-oligosaccharides.

Compound	**%, w/w**
monosaccharides	18,05
lactose	10,58
GOS-2	14,03
GOS-3	14,89
GOS-4	11,34
GOS-5	5,76
GOS-6	2,62
Proteins	0,09
Ash	1,01

Detection of saccharide oxidation products

After the conversion of saccharides in the model reactor, the samples were collected and analysed using high-performance liquid chromatography-mass spectrometry (HPLC-MS) system equipped with a mass spectrometer with an electrospray ionization (ESI) source. The chromatographic separation was conducted using a YMC Pack Pro column (3 x 150 mm; YMC) at 40°C and a mobile phase that consisted of 0.1% formic acid water solution (solvent A) and acetonitrile (solvent B) delivered in the isocratic (60% solvent B) elution mode. Mass scans were measured from m/z 50 up to m/z 1200 at a 350°C interface temperature, 250°C desolvation line (DL) temperature, ±4500 V interface voltage, and neutral DL/Q_{array}, using N_2 as nebulizing and drying gas. Mass spectrometry data were acquired in both positive and negative ionization

modes. Based on HPLC- MS analysis, the conversion of mono- and disaccharides resulted in the formation of a single product with a molecular mass that was 16 Da higher than that of the substrate (Fig. S5). In the reaction mixtures sampled before enzymatic oxidation, we did not identify any molecular ions typical for oxidation products (Fig. S6).

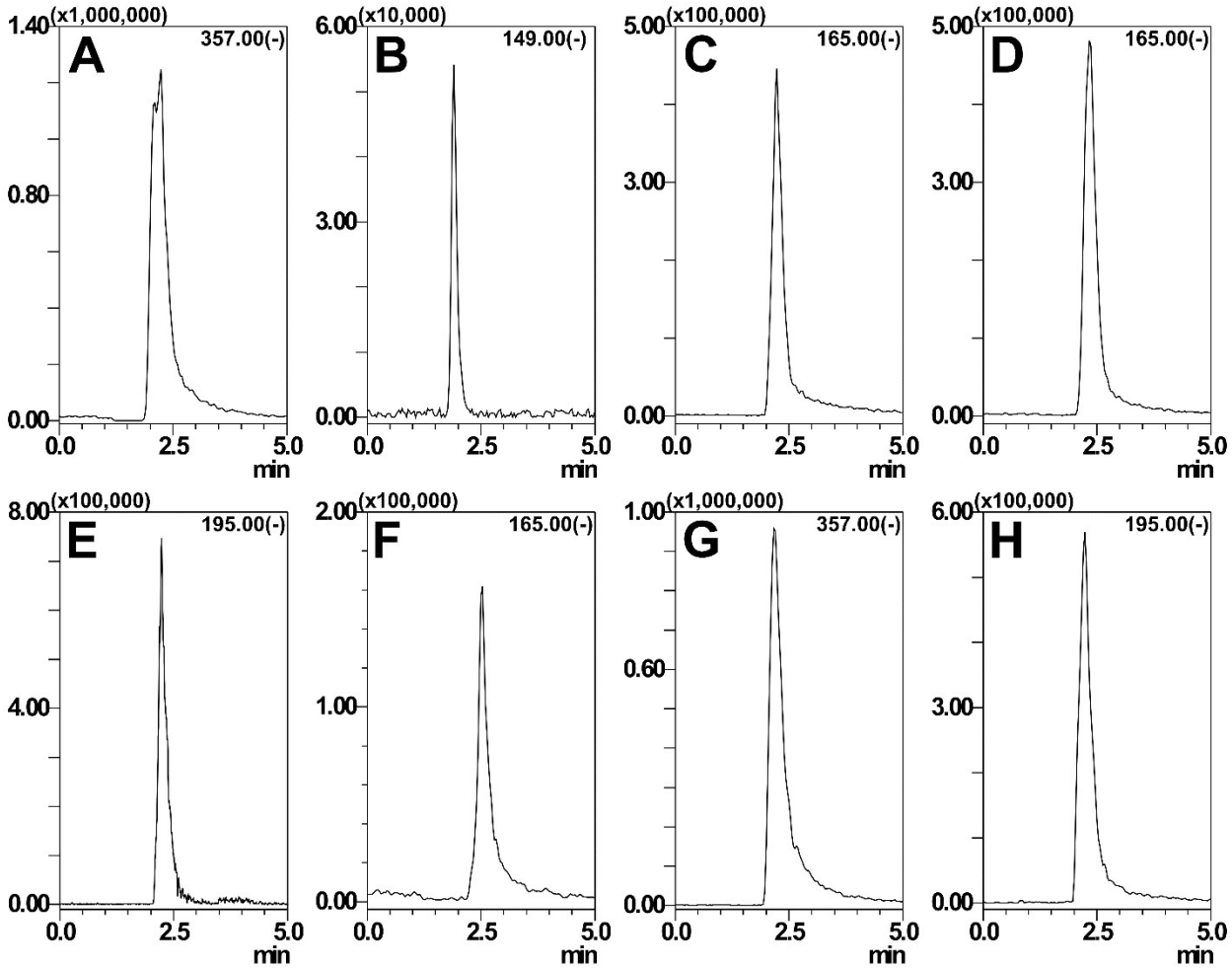

Fig. S4. HPLC-MS analysis of the reaction mixtures sampled after enzymatic oxidation of aldose sugars. Extracted ion chromatograms of oxidation products of (A) cellobiose, $[M-H]^-$=357; (B) deoxyribose, $[M-H]^-$=149; (C) ribose, $[M-H]^-$=165; (D) xylose, $[M-H]^-$=165; (E) glucose, $[M-H]^-$=195; (F) lyxose, $[M-H]^-$=165; (G) lactose, $[M-H]^-$=357; (H) galactose, $[M-H]^-$=195.

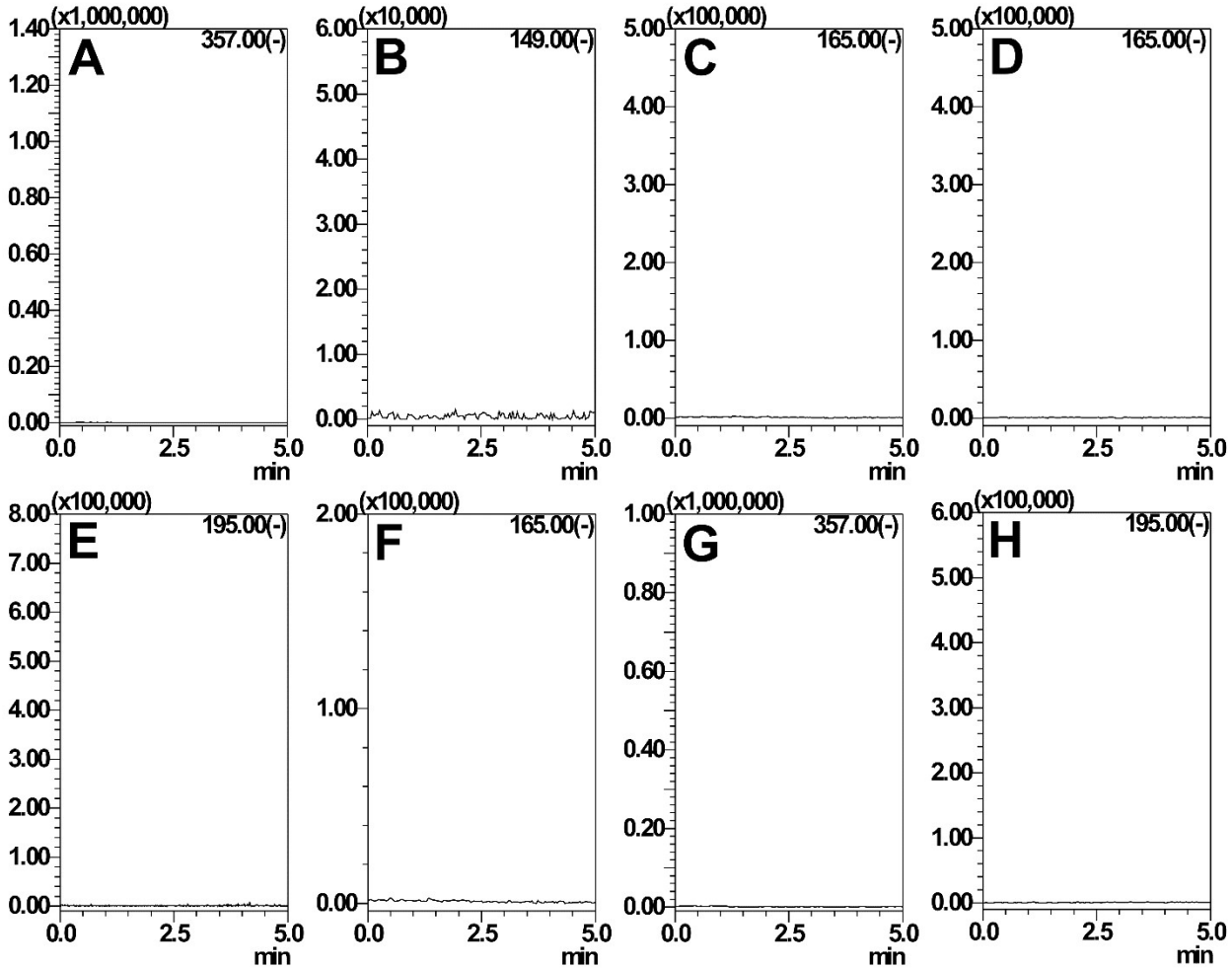

Fig. S5. HPLC-MS analysis of the reaction mixtures sampled before enzymatic oxidation of aldose sugars. Extracted ion chromatograms typical for (A) cellobiose, $[M-H]^-$=357; (B) deoxyribose, $[M-H]^-$=149; (C) ribose, $[M-H]^-$=165; (D) xylose, $[M-H]^-$=165; (E) glucose, $[M-H]^-$=195; (F) lyxose, $[M-H]^-$=165; (G) lactose, $[M-H]^-$=357; (H) galactose, $[M-H]^-$=195.

The HPLC analysis of the reactor mixtures showed that all the saccharides of the GOS mixture are oxidized, but the present of products is higher for short saccharides (mono- and disaccharides), and only very small part of long chain saccharides are oxidized (Fig. S7).

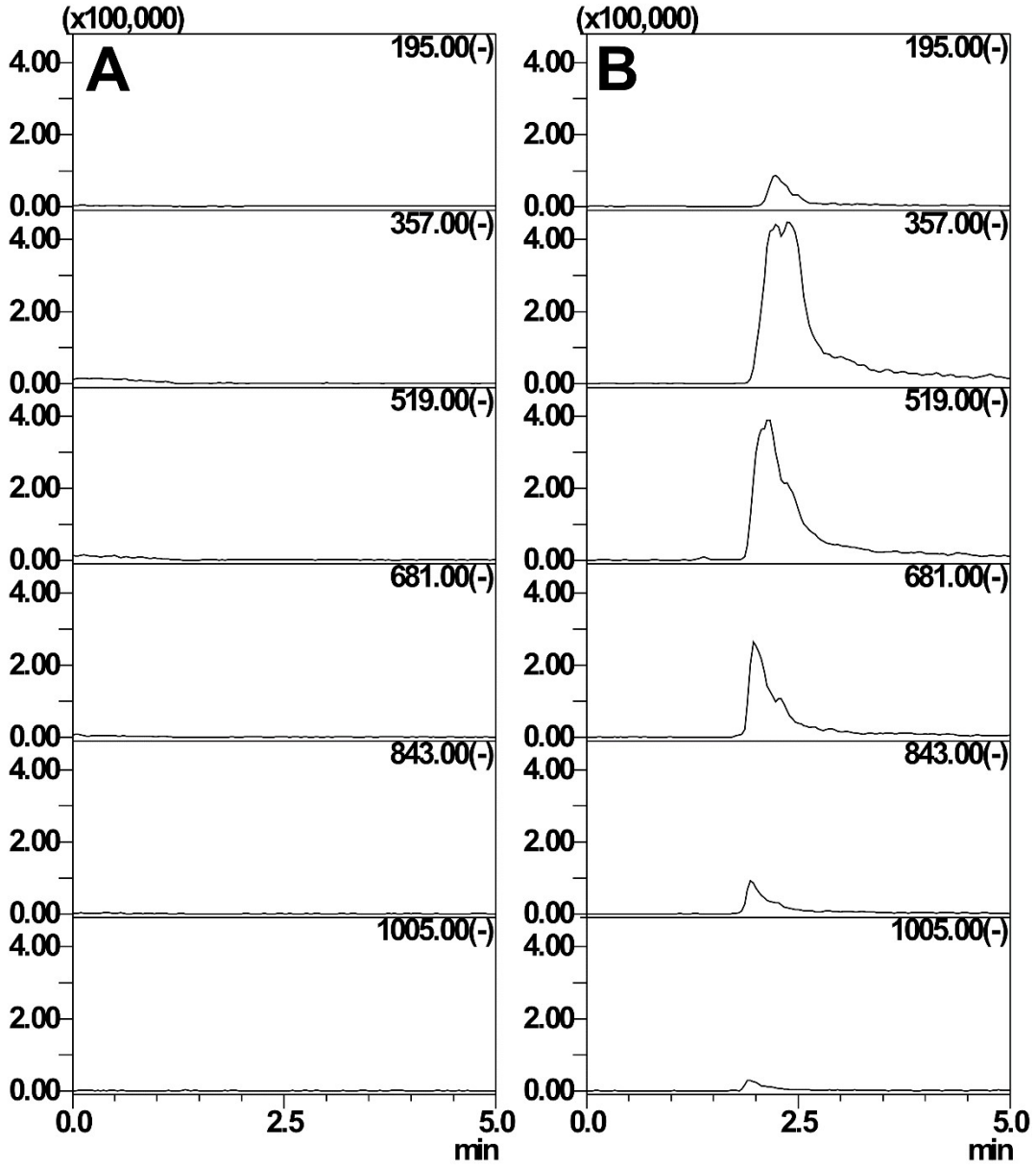

Fig. S6. HPLC-MS analysis of the reaction mixtures sampled before (A) and after (B) enzymatic oxidation of GOS mixture. Extracted ion chromatograms of oxidation products of aldohexose, $[M-H]^-$=195; lactose and GOS-2, $[M-H]^-$=357; GOS-3, $[M-H]^-$=519; GOS-4, $[M-H]^-$=681; GOS-5, $[M-H]^-$=843; GOS-6, $[M-H]^-$=1005.

NMR spectroscopy

NMR spectra were recorded in D_2O on Avance III 400: ^1H NMR – 400 MHz, ^{13}C NMR—100 MHz (Bruker, Billerica, OMA, USA). Chemical shifts (δ) are reported in parts per million (ppm). The multiplicities are stated as follows: s = singlet, d = doublet, dd = doublet of doublets, t = triplet, m = multiplet.

Identification of the products produced by enzymatic oxidation of aldose sugars

Deoxyribonic acid (Fig. S8–S9):

^{13}C NMR (101 MHz, Deuterium Oxide) δ **179.68 (C1),** 179.38, 88.82, **74.36 (C3), 69.57 (C4),** 68.14, **62.45 (C5),** 60.87, **40.17 (C2),** 37.61.

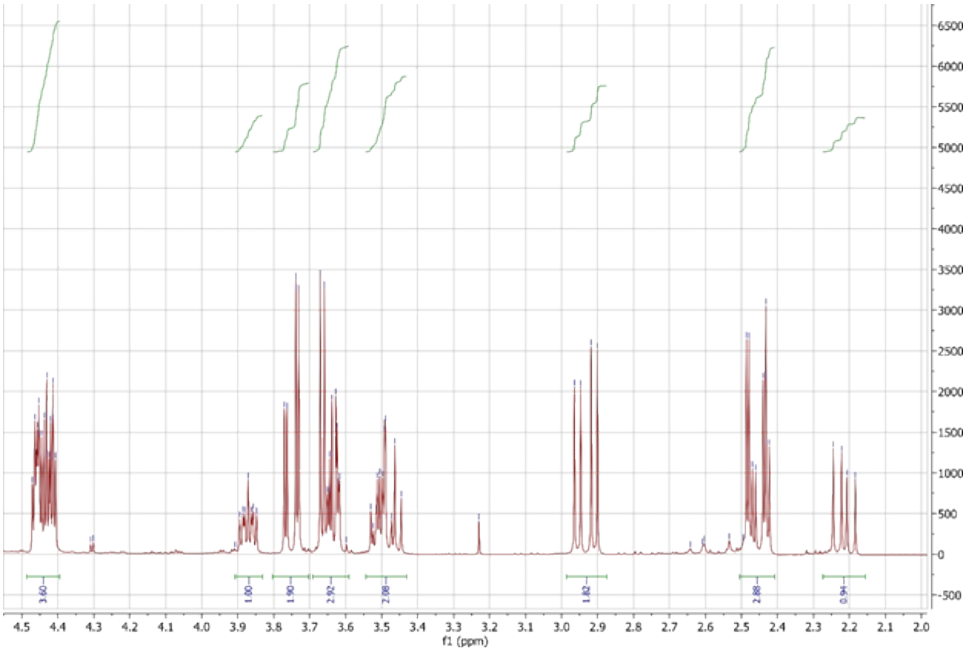

Fig. S7. ^{1}H-NMR of deoxyribonic acid.

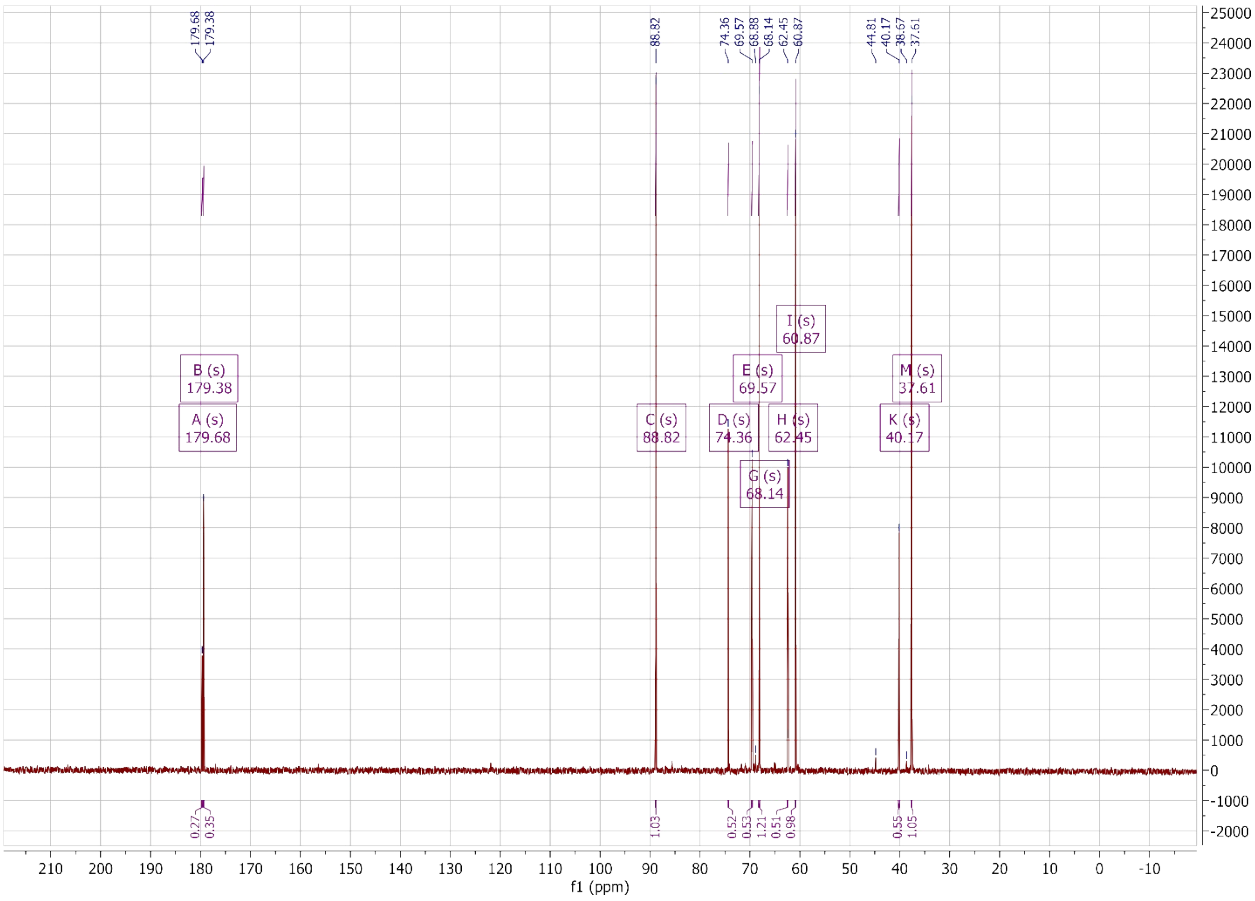

Fig. S8. ^{13}C-NMR of deoxyribonic acid.

Ribonic acid (Fig. S10–S11):

^{1}H NMR (400 MHz, Deuterium Oxide) δ 4.08 (d, J = 3.4 Hz, 1H), 3.80 (dd, J = 7.1, 3.5 Hz, 1H), 3.76 – 3.69 (m, 2H), 3.58 – 3.51 (m, 1H).

^{13}C NMR (101 MHz, Deuterium Oxide) δ 178.26 (C1), 73.57 (C2), 73.35 (C4), 71.60 (C3), 62.93 (C5).

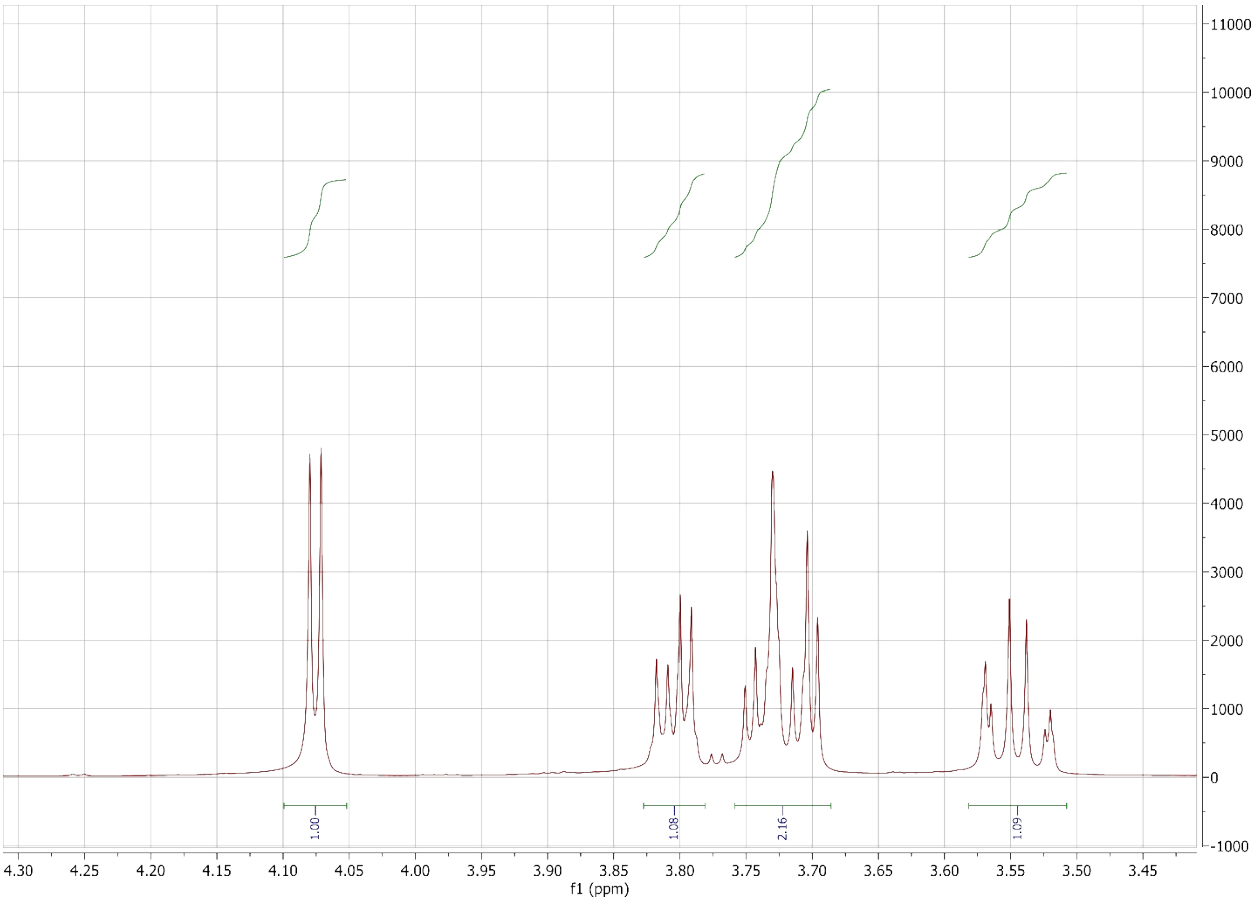

Fig. S9. ^{1}H-NMR of ribonic acid.

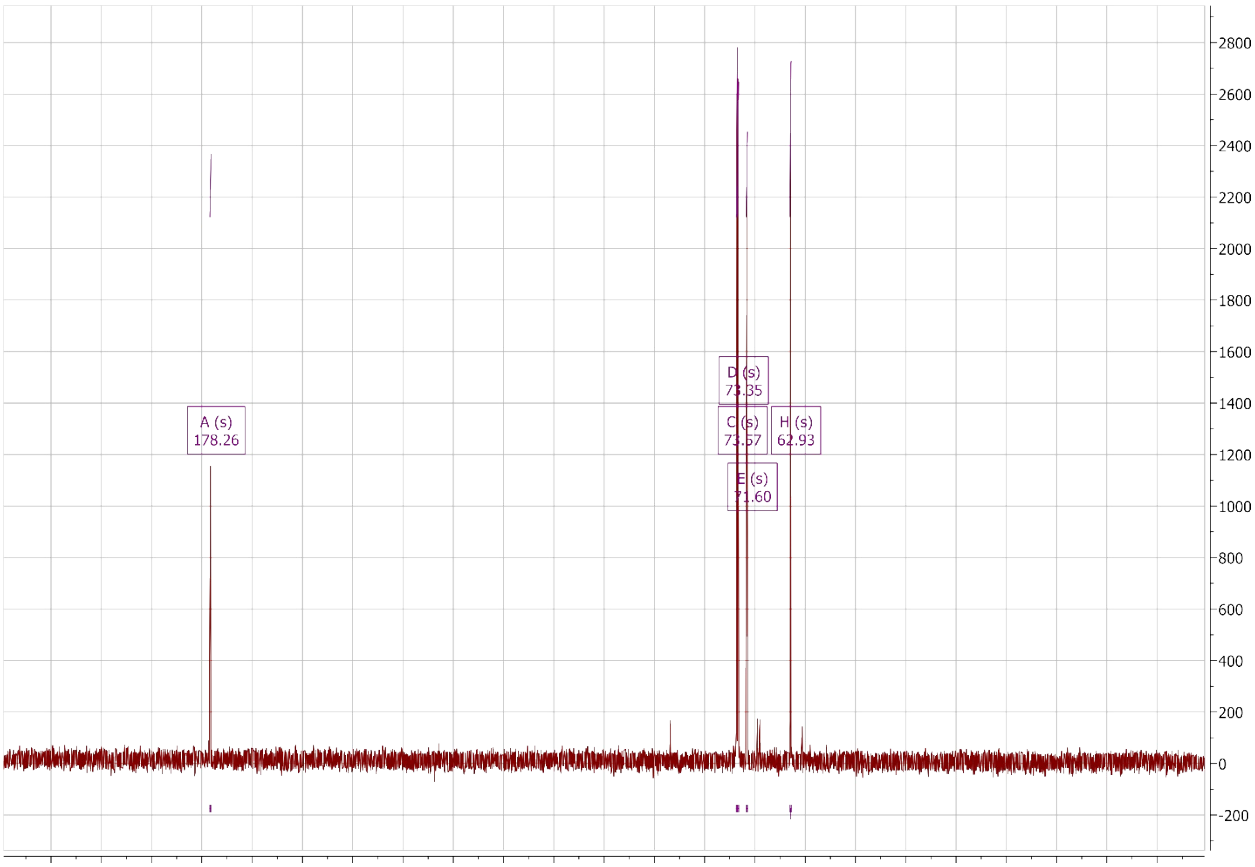

Fig. S10. ^{13}C-NMR of ribonic acid.

Xylonic acid (Fig. S12–S13):

^{1}H NMR (400 MHz, Deuterium Oxide) δ 3.94 (d, *J* = 2.6 Hz, 1H), 3.74 (dd, *J* = 6.4, 2.6 Hz, 1H), 3.67 (td, *J* = 6.4, 3.7 Hz, 1H), 3.61 (dd, *J* = 11.9, 3.7 Hz, 1H), 3.50 (dd, *J* = 11.9, 6.5 Hz, 1H).

^{13}C NMR (101 MHz, Deuterium Oxide) δ 178.57 (C1), 72.74 (C4, C2), 72.44 (C3), 62.44 (C5).

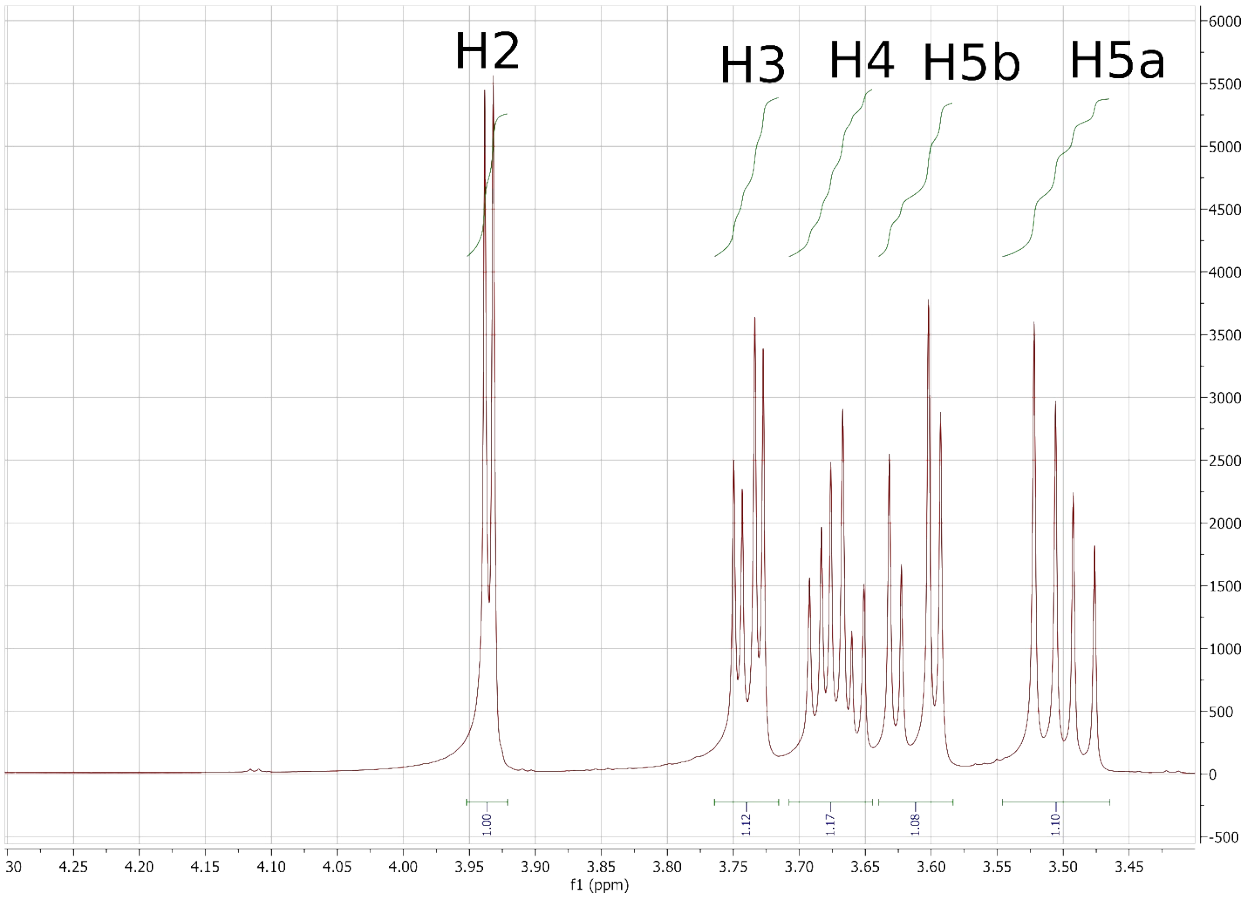

Fig. S11. ^{1}H-NMR of xylonic acid.

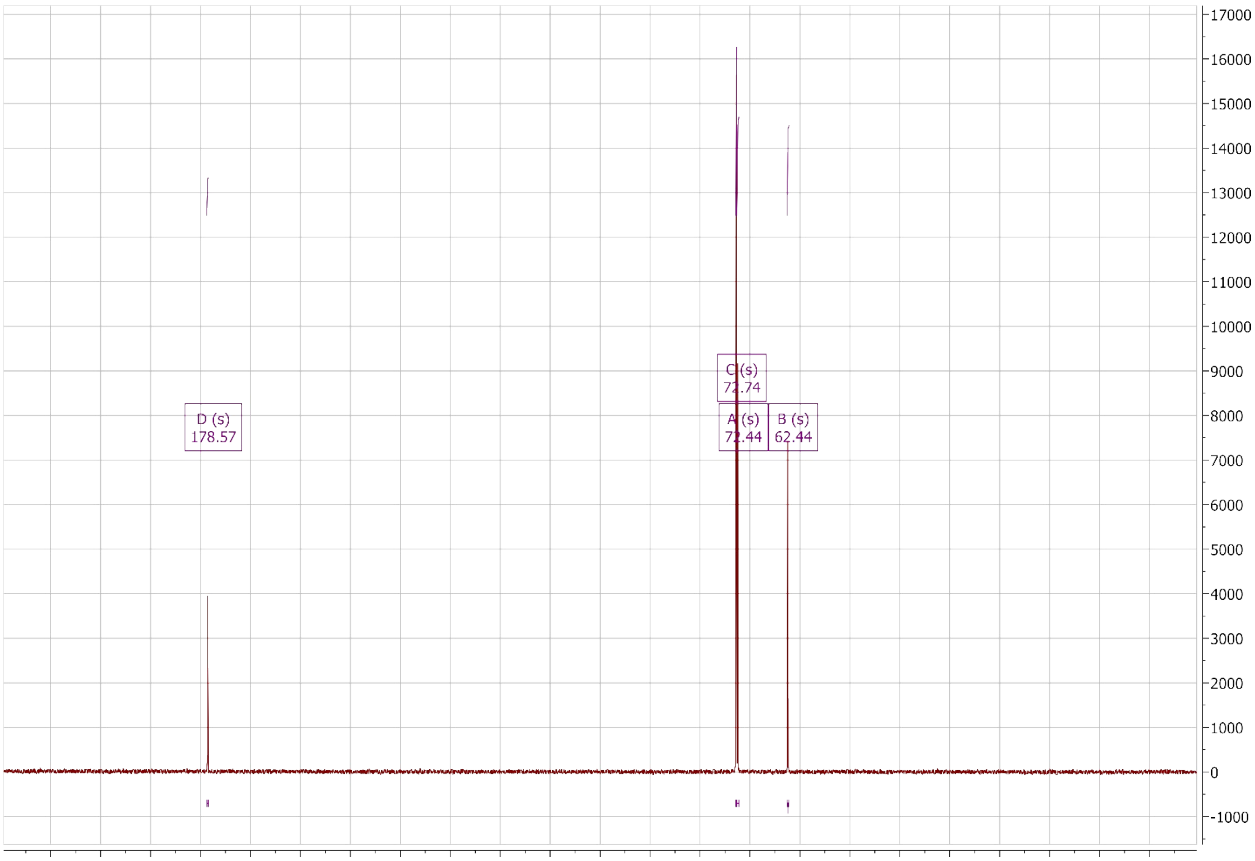

Fig. S12. ^{13}C-NMR of xylonic acid.

Gluconic acid (Fig. S14-S15).

^{1}H NMR (400 MHz, Deuterium Oxide) δ 4.02 (d, J = 3.7 Hz, 1H), 3.91 (t, J = 3.3 Hz, 1H), 3.80 – 3.67 (m, 1H), 3.71 – 3.61 (m, 2H), 3.64 – 3.48 (m, 1H).

^{13}C NMR (101 MHz, Deuterium Oxide) δ 178.59 (C1), 74.01 (C2), 72.51 (C4), 71.17 (C5), 70.96 (C3), 62.58 (C6).

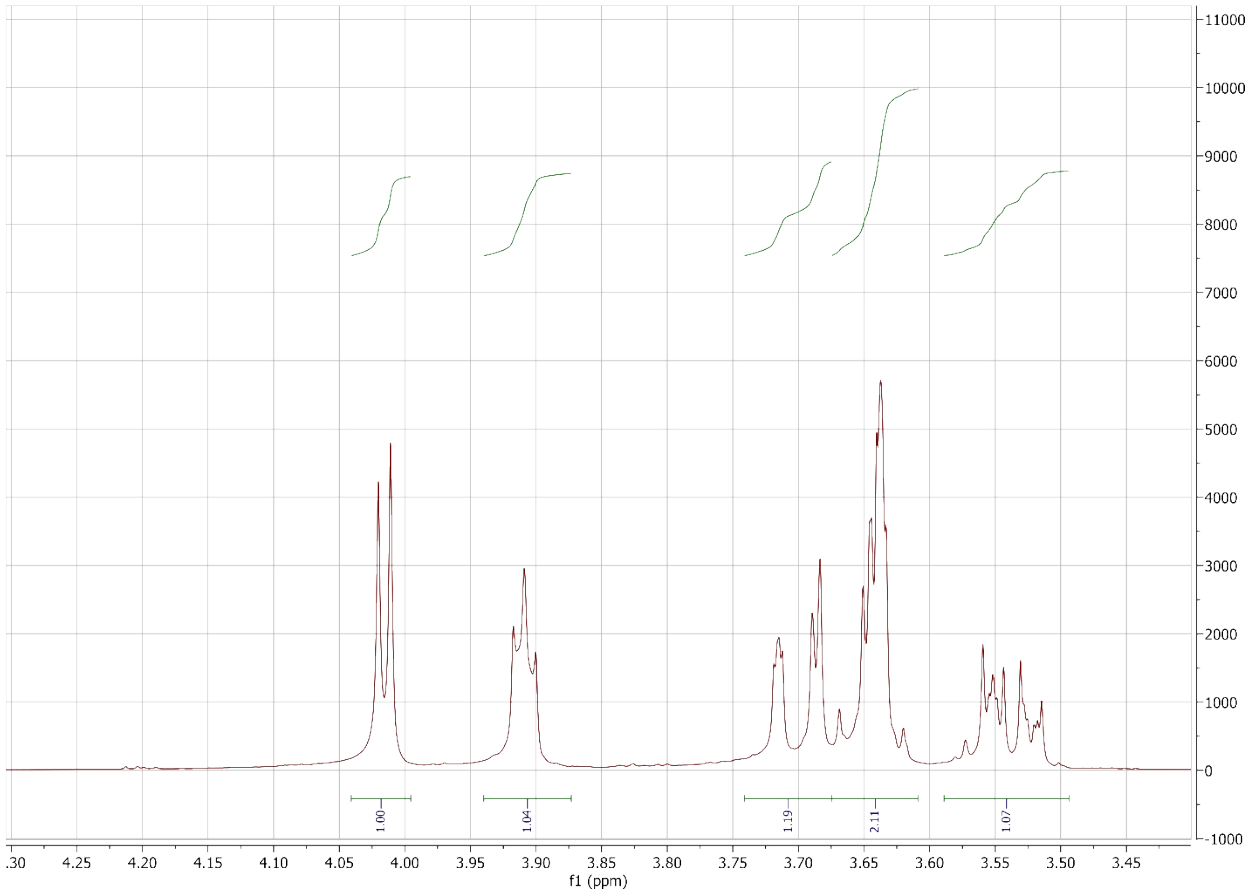

Fig. S13. ^{1}H-NMR of gluconic acid.

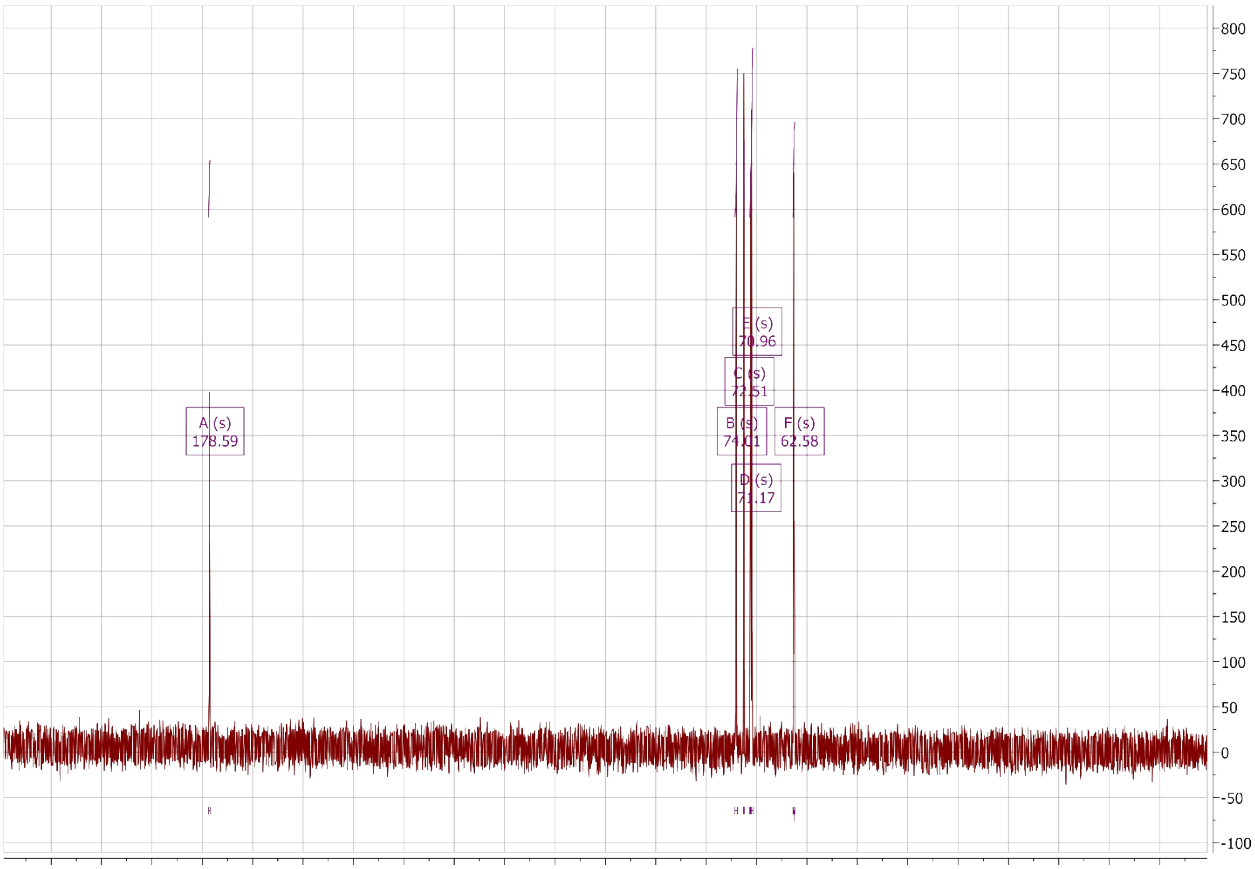

Fig. S14. ^{13}C-NMR of gluconic acid.

Lyxonic acid (Fig. S16–S17):

^{1}H NMR (400 MHz, Deuterium Oxide) δ 4.00 (d, *J* = 5.2 Hz, 1H), 3.77 (ddd, *J* = 7.6, 5.0, 2.9 Hz, 1H), 3.68 (dd, *J* = 5.2, 2.9 Hz, 1H), 3.58 – 3.47 (m, 2H).

^{13}C NMR (101 MHz, Deuterium Oxide) δ 178.75 (C1), 73.67 (C3), 71.80 (C2), 71.21 C4), 62.88 (C5).

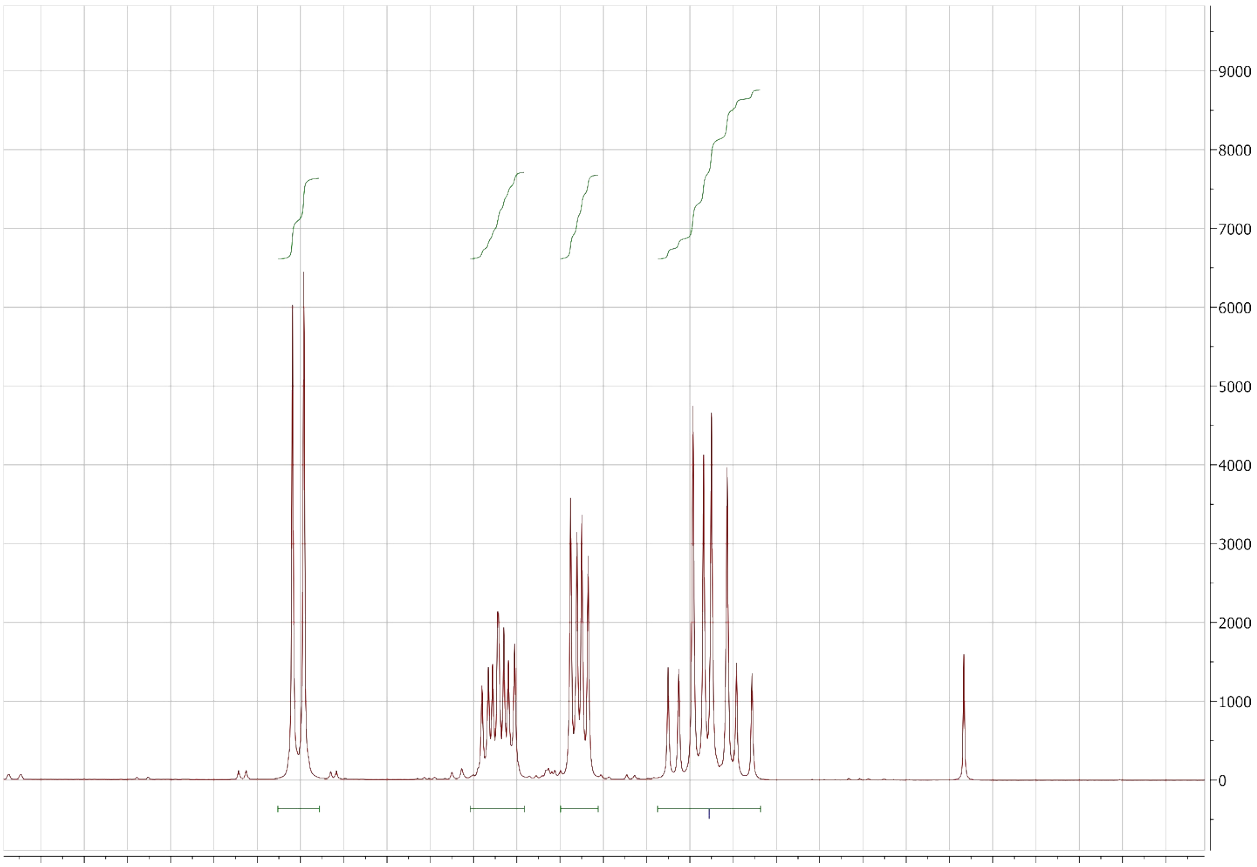

Fig. S15. ^{1}H-NMR of lyxonic acid.

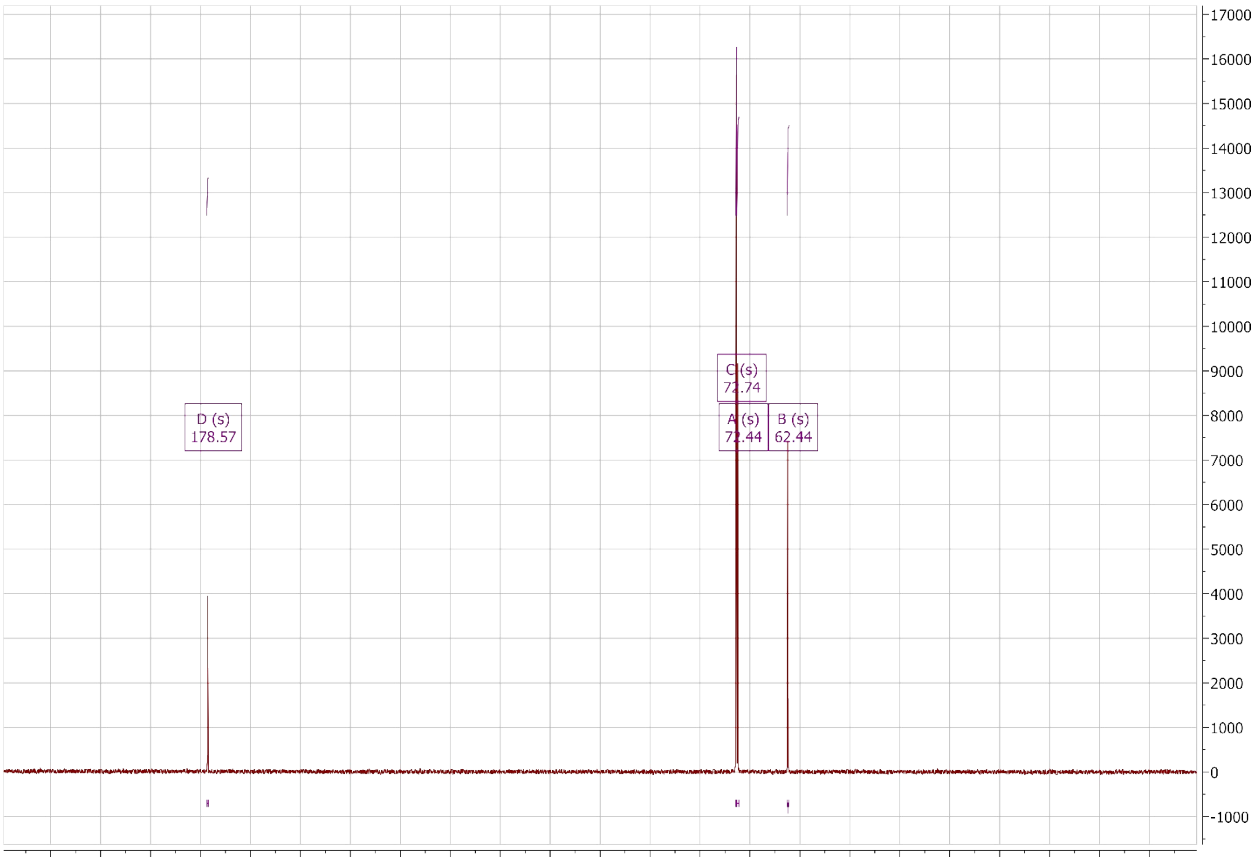

Fig. S16. ^{13}C-NMR of lyxonic acid.

References

1. J. Razumiene, I. Sakinyte, J. Barkauskas and R. Baronas, *Appl. Surf. Science*, 2015, **334**, 185.

2. M. Bausch, C. Schultheiss and J.B. Sieck, *Biotechnol. J.*, 2019, **14**, 1700721.